

# Zebrafish as a Universal *in vivo* Model for Plasmonic Nanoparticle Medicine

E. Lukianova-Hleb\*, C. Santiago\*\*, D. Wagner\*\*, J. Hafner\*\* and D. Lapotko\*,\*\*

\*A.V.Lykov Heat & Mass Transfer Institute,

15 P. Brovka St., Minsk, 220072, Belarus, hlebkate@yahoo.com

\*\*Rice University, 6100 Main Street, Houston, TX, 77005, USA, dmitri.lapotko@rice.edu

## ABSTRACT

The zebrafish embryo has been evaluated as an *in vivo* model for plasmonic nanobubble (PNB) generation and detection at nanoscale. The embryo is easily observed and manipulated utilizing the same methodology as for application of PNBs *in vitro*. Injection and irradiation of gold nanoparticles with a short laser pulse resulted in generation of PNBs in zebrafish with the similar parameters as for PNBs generated in water and cultured living cells. These PNBs do not result in systemic damage, thus we demonstrated *in vivo* model for rapid and precise testing of plasmonic nanotechnologies.

**Keywords:** zebrafish, laser, gold nanoparticles, plasmonic nanobubbles.

## 1 INTRODUCTION

*In vivo* application of plasmonic methods faces serious challenges because standard animal models are not well suited for optical activation and detection of plasmonic effects and for precise control the distribution and interactions of the nanoparticles (NP) with a host. With the aim of developing an efficient *in vivo* model for plasmonic nanomedicine we have evaluated zebrafish. Zebrafish is the vertebrate organism that is relatively optically transparent, develops quite fast and physiologically is similar to human. Zebrafish has already been evaluated as a model for analysis of the distribution and toxicity of plasmonic (gold) NPs [1-3] and also has allowed efficient optical manipulations including laser microsurgery and sensing [4-8].

We have hypothesized that zebrafish can be used as an efficient *in vivo* model for the development of the cell level plasmonic nanotechnologies for the diagnostics, therapy and theranostics (combined diagnosis and therapy). This hypothesis has been tested experimentally with the focus on the two tasks: optical generation and detection of the single localized plasmonic events in living zebrafish, and on the safety of the NP targeting, activation and detection. We have used single short laser pulse excitation of vapor nanobubbles around gold NPs [9]. This mode of plasmonic interaction may provide a single cell selectivity of therapeutic (mechanical) effect [10, 11] and the sensitivity of optical scattering imaging being 10-100 times higher than the sensitivity of the gold NP scattering methods [12,13]. Most important, the properties of plasmonic

nanoparticle-generated vapor bubbles (plasmonic nanobubbles - PNB) can be dynamically tuned from non-invasive to damaging modes through the fluence of the pump laser pulse.

## 2 MATERIALS AND METHODS

### 2.1 Zebrafish

Zebrafish were maintained in accordance with protocols approved by the Rice University Institutional Animal Care and Use Committee. Zebrafish were maintained at 28°C in recirculating water systems (Aquatic Habitats) in 14 hours light 10 hours dark. 30 hour post fertilization embryos (hpf) were imbedded in 1% low melt agarose (#A-9045, Sigma-Aldrich Corp., St. Louis, MO). 60 nm diameter gold spheres (#10-B-100, Nanopartz, Salt Lake City, UT) were used in experiments. 4 nL of  $2.6 \cdot 10^{10}$  particles/ mL was injected subcutaneously into the flank at the level of the end of the yolk extension. Successful injection was monitored by local inflation of the skin. Embryos were removed from low melt agarose and placed in embryo medium (E3) in bridged coverslips. Injected embryos and mounted uninjected embryos were subjected to PNB induction in multiple locations around and distant to the injection site. Embryos were removed from the bridged coverslip and monitored for survival. Injected PNB induced embryos survived to 9 days post fertilization, developed swim bladders and showed no obvious defects associated with treatment.

### 2.2 Cells

For the tissue culture based *in vitro* experimental model we have used the same gold spheres. The cells were prepared as the monolayers of living isolated lung carcinoma cells (A549) that were grown into standard 6-mm culture wells (#C24765, Molecular Probes, Inc., Eugene, OR). All cells were incubated with NPs for 60 min at 37°C. The concentration of the NPs during the incubation was adjusted to  $0.2-0.9 \cdot 10^{11}$ /ml. During non-specific endocytosis the NPs were internalized and concentrated into the clusters of closely packed NPs in endosomal compartments, as we have shown earlier [11,14]. Cell viability was evaluated optically with two standard microscopy techniques. First, a bright light image was obtained for the cell before and after its exposure to pump

pulse and the difference of these two images was used to detect any PNB-induced changes of the shape of the cell, in particular, emerging of the blebbing bodies. Second, the membrane damage by PNB was detected using standard fluorescent method by monitoring the cellular uptake of ethidium bromide (EtBr) dye. Fluorescent images were obtained for each cell before and after their exposure to the pump laser pulses.

### 2.3 Optical generation and detection of PNBs

PNBs were generated by laser pulse-heating of gold NPs. In our work we have employed a pulse of length 0.5 ns, 532 nm (STA-01 SH, Standa Ltd, Vilnius). The pump laser beam was directed into the illumination path of an inverted optical microscope and was focused into the sample. Laser beam diameter was 14  $\mu\text{m}$  in the sample plane. Single events were studied. PNB detection has been realized with two optical methods that take advantage of the excellent optical scattering properties of bubbles [14]. The time-resolved imaging of NPs and PNBs was realized by using side illumination of the sample with a custom made pulsed probe dye laser beam at a wavelength (690 nm, 0.5 ns, dye laser) and with a tunable time delay of 1-10 ns relative to the pump pulse. The scattered probe radiation was imaged with a digital camera (Luka, Andor Technologies, Ireland). For quantitative analysis of the optical amplification we have employed differential images:  $S_{sc}(t) = [I(t) - I_b]$  that describes the pixel image amplitude  $I(t)$  of optical scattering by a transient PNB and compensates for the stationary scattering from the background (cell, tissue). While allowing us to image and quantify the PNB the pulsed imaging can hardly provide kinetic measurement. The latter was realized by the thermal lens method in a response mode. An additional continuous probe beam (633 nm) was directed at the sample and focused on it collinearly with probe laser beam and its scattered by PNB component was monitored by a high-speed photodetector (PDA510, Thorlabs Inc.) (Figure 1).

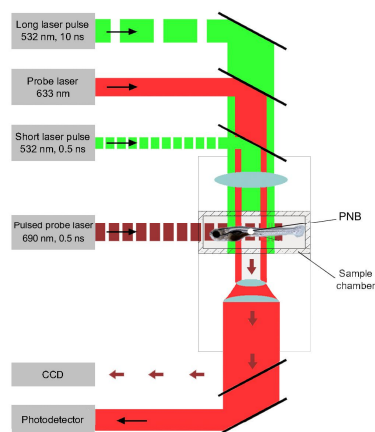


Figure 1: Experimental setup: single gold NPs in water or individual cells in the sample chamber were mounted on the stage of inverted optical microscope; PNB generation was

provided by focused single pulses (532 nm, 0.5 ns); a pulsed probe laser (690 nm, 0.5 ns) provided time-resolved optical scattering imaging of PNB and a continuous probe laser (633 nm, 1 mW) provided the monitoring of the integral optical scattering of PNBs through their time-responses. Additional pulsed laser (532 nm, 10 ns, 1  $\text{mJ}/\text{cm}^2$ ) was used for excitation of fluorescence in the cells.

The response mode allowed measurement of the PNB lifetime that characterizes a maximal diameter of the bubble. Image and response modes were used simultaneously thus combining the imaging and measuring of the lifetime (Figure 1). An additional pulsed laser (532 nm, 10 ns, LS 2132 by Lotis TII, Minsk) was used for the excitation of red fluorescence from ethidium bromide dye. The fluence of this laser was set at the level well below PNB generation threshold (that is quite high for such long pulses).

We used the zebrafish to assay for PNB generation *in vivo* (Figure 2).

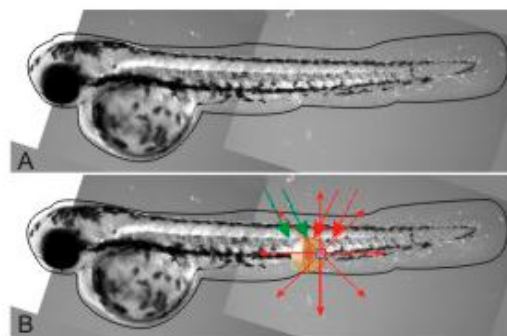


Figure 1: Zebrafish model for PNB generation and detection. A: bright field image of the embryo; B: PNB is generated (with green pump laser pulse) and detected (with red probe laser pulse) thus sensing the cell.

## 3 RESULTS

A549 lung carcinoma cells were incubated for 60 min at 37°C with the same gold NPs as have been used in the above experiments. Then individual cells were irradiated with single pump laser pulses at various fluence levels. We measured the PNB generation threshold fluence, dependence of the PNB lifetime and scattering image amplitude upon the pump laser fluence and the viability of the cells after their exposure to laser pulse (with 60 s delay). For each cell we have registered bright field and side scattering optical images before and after the pump laser pulse (Figure 3). The lifetime of PNBs detected in the cells under the pump laser fluence of 200  $\text{mJ}/\text{cm}^2$  was  $50 \pm 21$  ns, which was longer than that for individual NPs under the same laser fluence ( $23 \pm 13$  ns). The amplitudes of PNB scattering images obtained at this fluence were close to those obtained for NP clusters in water. Furthermore, the PNB threshold fluence as measured for the NP-treated cells ( $0.09 \pm 0.03 \text{ J}/\text{cm}^2$ ) was found to be lower than the PNB generation threshold for single NPs ( $110 \text{ mJ}/\text{cm}^2$ ) [15]. These results allowed us to conclude that the PNBs have

been generated in cells around NP clusters and not around single NPs.

Optical scattering amplitudes of the PNBs were compared to those for gold NPs in the cells (without exposure to pump laser pulse). According to our data the PNBs have significantly amplified optical scattering of gold NPs:  $500 \pm 100$  for NPs and  $10000 \pm 455$  for PNBs, thus improving the sensitivity of PNB as optical probes by more than one order of magnitude relative to NPs. Detection of cell damage was based on the fluorescent registration of the uptake of a cell impermeant dye, ethidium bromide, and additionally, on the registration of the blebbing bodies in the bright field images of the cells after the pulse (Figure 3c). Dye-specific signals have been detected within 60 s after the treatment of the cell with a single laser pulse and accompanying PNB.

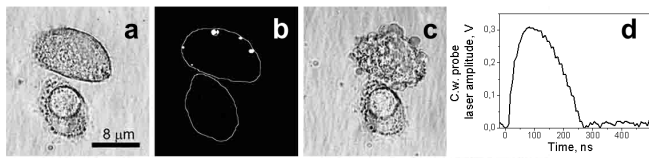


Figure 3: *In vitro* generation and detection of PNB in gold NP-treated A 549 cells: (a): bright field microscopy image of 2 cells prior to their exposure to a single pump laser pulse (532 nm, 0.5 ns, 200 mJ/cm<sup>2</sup>); (b): time-resolved scattering image of the intracellular PNBs obtained with the delayed for 10 ns (relative to the pump laser pulse) pulsed probe laser (690 nm, 0.5 ns), white lines show the contours of the cells as in (a); (c): bright field microscopy image of 2 cells obtained 120 s after their exposure to a single pump laser pulse and the generation of the PNBs; (d): time-response obtained during the exposure to a single pump laser pulse shows the bubble expansion and collapse, the baseline after the bubble collapse shows the noise of the probe laser.

We have found that the cell damage was correlated to the level of the pump laser fluence and to the PNB lifetime: cells have not been damaged by the pump laser pulses with the fluence below 1.0 J/cm<sup>2</sup> and by the corresponding PNBs with the lifetime below 110 ns. Thus the PNB generation threshold in living cells was almost 10 times lower than the cell damage threshold fluence. Since the PNB lifetime is determined by maximal size of the PNB and depends linearly on the fluence of the pump laser pulse, we may assume that the observed laser-induced damage of the cells was related to the PNB size. The viability of the adjacent cell was also verified by the absence of damage-specific fluorescence (unlike in the neighboring cell that has yielded the PNBs and later has produced a damage-specific fluorescence).

We applied the aqueous and cell culture PNB methods to the zebrafish and determined the optical and mechanical properties of PNBs *in vivo*. We injected 60 nm gold nanospheres into the flank of 1 day post fertilization embryos. We irradiated the embryos with the same single short laser pulses (532 nm, 0.5 ns, 200 mJ/cm<sup>2</sup>) on the same

apparatus that we used to generate PNBs *in vitro*. We irradiated several points located inside and outside NP injection area (Figure 4a). We registered bright field and side scattering images of each point prior to their exposure to the pump laser pulse. Next, we have recorded side scattering image of the same area with 10 ns time delay relative to the pump pulse and have subtracted previous scattering image. The resulting differential image (Figure 4b) clearly showed PNBs which also had a time-response signal with a shape typical for PNB (Figure 3d-I,II). PNBs were detected only within the injection area while no PNBs were detected outside this area (Figure 3III-b,d). Lifetimes of PNBs varied among sampled points (inside injection area) from 20 ns up to 700 ns at the fixed laser pulse fluence of 200 mJ/cm<sup>2</sup>. This range corresponds to the PNB lifetime observed for single NPs at low end and NP clusters which yield much longer PNBs. Therefore, the PNB detected in zebrafish show the same response as we observe from cultured cells and have been generated by single NPs and by their clusters (Figure 3d-I) (depending upon actual aggregation state of the NPs after their injection).

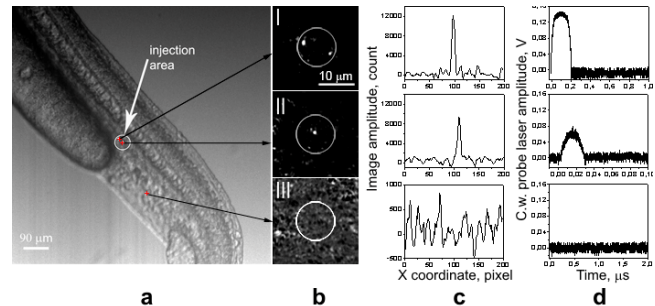


Figure 4: (A): bright field microscopy image of zebrafish embryo shows gold NP injection area (white circle) and several numbered irradiation points where single pump laser pulses were applied; (b): time-resolved scattering differential images of three numbered points obtained with the delayed for 10 ns (relative to the pump laser pulse) pulsed probe laser (690 nm, 0.5 ns), white circle shows the aperture of the pump laser beam; (c): profiles of the pixel image amplitudes for the corresponding images in (b) (1  $\mu$ m is 14 pixels); (d): corresponding time-responses obtained during the exposure to the pump laser pulse shows the bubble expansion and collapse, the signal after the bubble collapse is identical to the baseline, note different time (X) and output signal (Y) scales.

Optical scattering images related to the PNBs were also detected only within the injection area. PNB-related amplitudes in the light scattering images were well above the tissue-generated background scattering (Figure 4c-III):  $12000 \pm 655$  and  $200 \pm 25$  correspondingly, while the scattering from the corresponding NPs (without their exposure to the pump laser pulse) was weaker or comparable to the tissue scattering and did not exceed the background scattering (Figure 4c). Therefore, PNBs as optical probes were much brighter than NPs, and were

detectable in living tissue under conditions when the NPs could not be detected due to the strong background scattering.

Analysis of the PNB lifetimes indicated that *in vivo* and *in vitro* generated PNBs are likely to be generated by NP clusters that may form in cells and after the injection in zebrafish. The level of optical scattering amplitudes for the *in vivo* and *in vitro* generated PNBs were close to each other and their level also corresponded to NP clusters rather than to the single NPs (Figure 4c). Therefore, we may suggest that the signals observed in NP-treated zebrafish were associated with the generation of plasmonic nanobubbles around the clusters of gold NPs and were not accompanied by thermal effects such as hyperthermia or else. No large scale tissue disruption or alteration has been detected in bright field images of the zebrafish after generating the PNBs. The viability of each individual specimen has been monitored until 9 dpf. We have used several control samples (intact, anesthetized and unmounted; intact, anesthetized and mounted; injected, anesthetized and mounted, but not irradiated) so to exclude possible influence of the preparation steps on the viability. Each group has counted from 2 to 9 identical zebrafish. With one exception for a NP injection control all other experimental stages (including laser treatment and the generation of PNBs) have not caused any lethality. Therefore, generation and detection of plasmonic nanobubbles by itself is not lethal. This observation provides us with wide opportunities for using zebrafish as an *in vivo* platform for evaluating diagnostic and therapeutic methods based on plasmonic interactions.

Based on these results we assumed at least 3 modes of the PNB application *in vivo*:

1. Non-invasive diagnosis: single PNB with the lifetime below 110 ns can be detected and does not damage individual cells or tissues and does not influence animal viability;
2. Local (cell level) therapy: single PNB with the lifetime 110 – 700 ns damages individual cells (where it is generated), its optical scattering signal is damage-specific although such PNB does not disrupt the tissues and does not influence animal viability;
3. Tissue surgery: single or multiple PNBs with the lifetime above 700 ns disrupt the tissue and may not be safe for an animal.

The reported work has combined the unique properties of zebrafish such as optical transparency, compatibility with gold nanoparticles and ability to deliver and collect optical radiation. To the best of our knowledge this combination has resulted in the first non-invasive application of localized plasmonic processes in zebrafish. Application of gold nanoparticles, laser radiation and the generation of plasmonic nanobubbles (including those that caused the damage at cell level) did not compromise the short term viability of zebrafish. The diagnostic mechanism of plasmonic nanobubbles is based on amplification of

optical scattering and has provided high sensitivity for the noninvasive and localized detection of gold nanoparticles *in vivo*. The therapeutic mechanism of plasmonic nanobubbles is based on their mechanical, nonthermal action that can be localized to individual cells and cause their damage through the immediate disruption of the target cells while such bubbles do not damage a host (zebrafish) due to their transient and localized nature.

## REFERENCES

- [1] L. M. Browning, K. J. Lee, T. Huang, P. D. Nallathambiy, J. E. Lowman and X.-H. Na. Xu, *Nanoscale*, 1, 138, 2009.
- [2] R. J. Griffitt, K. Hyndman, N. D. Denslow and D. S. Barber, *Toxicological Sciences*, 107, 404, 2009.
- [3] Bar-Ilan, R. M. Albrecht, V. E. Fako and D. Y. Furgeson, *Small*, 5, 1897, 2009.
- [4] M. Sakakura, S. Kajiyama, M. Tsutsumi, J. SI, E. Fukusaki, Y. Tamaru, S.-I. Akiyama, K. Miura, K. Hirao and M. Ueda, *Jpn. J. Appl. Phys.*, 46, 5859, 2007.
- [5] V. Kohli and A. Y Elezzabi, *BMC Biotechnology*, 8, 7, 2008.
- [6] A. Jorgensen, J. E Nielsen, J. E Morthorst, P. Bjerregaard and H. Leffers, *Reproductive Biology and Endocrinology*, 7, 97, 2009.
- [7] K. S. Liu and J. R. Fetcho, *Neuron*, 23, 325, 1999.
- [8] M. C. Halloran, M. Sato-Maeda, J. T. Warren, Jr, Fe. Su, Z. Lele, P. H. Krone, J. Y. Kuwada and W. Shoji, *Development*, 127, 1953, 2000.
- [9] D. Lapotko, *Opt. Express*, 17, 2538, 2009.
- [10] E. Y. Hleb, J. H. Hafner, J. N. Myers, E. Y. Hanna, B.C. Rostro, S. A. Zhdanok and D.O. Lapotko, *Nanomedicine*, 3, 647, 2008.
- [11] D. Lapotko, E. Lukianova, M. Potapnev O. Aleinikova and A. Oraevsky, *Cancer Lett.*, 239, 36, 2006.
- [12] E. Y. Hleb, Ying Hu, R. A. Drezek, J. H. Hafner and D. O. Lapotko, *Nanomedicine*, 3, 797, 2008.
- [13] E. Lukianova-Hleb and D. Lapotko, *Nano Letters*, 9, 2160, 2009.
- [14] D. Lapotko, *Nanomedicine*, 4, 813, 2009.
- [15] E. Y. Hleb, Y. Hu, L. Latterini, L. Tarpani, S. Lee, R. A. Drezek, J. H. Hafner and D. O. Lapotko, *ACS Nano*, doi10.1021/nn1000222, 2010.